

Comparison on Performance of Grid Connected DFIG-WT System using B2BC and NSC

^{1*}Subir Datta, ²Subhasish Deb, ³Ksh. Robert Singh

¹²³ Department of Electrical Engineering, Mizoram University, Aizawl, Mizoram, India

*subirnerist@gmail.com

<https://doi.org/10.26782/jmcms.2019.04.00022>

Abstract

This paper presents a comparative study of the performances of a doubly fed induction generator (DFIG) based grid connected wind turbine (WT) system using back-to-back converter (B2BC) and nine-switch converter (NSC). The time domain simulink results of the system variables, under varying wind velocity, are presented and analyzed all the results in details. Results show that the B2BC-used with DFIG-WT system can be replaced by NSC under any wind speed.

Keywords: WECS, DFIG, B2BC and NSC.

I. Introduction

Now-a-days, DFIG has become very popular in the application of the WT system due to its advantages over other wind turbine generators (WTGs). The some advantages are: (i) partially rated power converters are required as they handle only slip times of stator power, (ii) converter cost is low, (iii) lesser the injection of harmonics due to low rating of power converters, (iv) overall energy conversion efficiency is high, (v) possibility of decoupled control of active and reactive powers etc [II, VIII, XI, XII, XIII, XVII, XXIII]. Furthermore, loss minimizations and cost reduction are become the main concerned of many applications. Therefore, many attempts were taken in that direction to reduce the number of power semiconductors through topological modification in the converter. In [X, XVIII], matrix converter, comprising of nine bi-directional switches, is used in DFIG-WT system. But, the switching strategies based on classical PWM technique is not suitable for this type converter due to the limitation of switching frequency and requirement of additional auxiliary clamping circuit [V]. In [XVI], another topology comprising of two B4 converters, each comprising of four switches, is introduced for energy conversion of DC-AC or AC-DC [VI]. This reduces the number of switches to eight, but suffers from large voltage variation across the DC-link capacitor. In order to overcome this limitation, another converter was introduced, named as five-leg converter [IX, XIV]. In [III, IV, VII, XXI, XXIII], a competitive alternative converter of the existing B2BCs is introduced, called as Nine Switch Converter (NSC). It has only nine power semiconductor switches, which decrease the IGBT based component count, cost of power converter and switching losses of the

converter, and thereby the system efficiency is also increased. Unlike matrix converter, the NSC can be modulated by switching strategy based on classical PWM technique. NSC has been reported in [XXI], used as two separate converters, for controlling two AC loads separately. In [III, IV, XXI], NSC is used in different frequency (DF) based dual motor drives and common frequency (CF) based AC-AC converter applications. In [VII, XXIII], various types of modulating techniques are proposed for NSC. The grid connected DFIG-WT system with B2BC and NSC has been developed in MATLAB/Simulink environment and their performances under different wind velocity are studied in this paper. The time domain responses of the study system, obtained using B2BC, are compared with that of NSC. The simulink results show that NSC can also be an alternative reduced converter topology for WT system instead of B2BC. This paper is organized as follows: section-II illustrates the DFIG-WT system with B2BC. NSC based DFIG-WT system is presented in section-III. The control scheme for NSC is discussed in section-IV. The simulation results of the study system are discussed in section-V. Finally, conclusion is drawn in section-VI.

I. DFIG-WT SYSTEM WITH B2BC

Fig.1 shows the block diagram of the overall system of a B2BC based grid-connected DFIG-WT system along with the control scheme. Stator windings of the DFIG are directly connected to the power grid whereas the rotor windings are connected to the same power grid, but through a conventional B2BC, comprising of Rotor Side Converter (RSC) and Grid Side Converter (GSC), connected through dc-link capacitor [II].

Rotor speed (ω_r) of DFIG is controlled and set to the desired value (ω_{ref}) by controlling the direction and magnitude of active power flow (P_r) through its rotor so that WT can extract the highest amount of power (P_{opt}) from the wind of certain velocity. Corresponding to any wind speed, P_{opt} value is obtained from the optimum power versus wind-speed curve and is considered as the reference or set active power. Actual value of active power extracted/converted into electrical power (P_s) is continuously calculated from the measured data, controlled by controlling P_r and is used to track the reference active power (P_{opt}). Once, set active power is reached, the desired rotor speed is automatically achieved.

To control of stator active and reactive power independently, stator field oriented reference frame has been used. RSC is controlled to get control over rotor d- and q-axis current components. In stator field-oriented vector control, stator and rotor components are transformed to a synchronously rotating reference frame, where the d-axis components of stator magnetic flux is aligned on the reference frame (d-axis) of the synchronously rotating reference frame. This field oriented vector scheme is considered to design the control scheme of RSC of DFIG. The details of the control strategy of the B2BC based grid connected DFIG-WT system are described in the [XIX].

II. DFIG-WT SYSTEM WITH NSC

NSC based DFIG-WT system is shown in Fig.2. It uses three IGBT switches in series for each phase, requiring nine switches in total. The switch count of power converter is decreased by 50% and 33% respectively in contrast to conventional matrix converter and 12-switch B2B converter [III], as middle switches of NSC are shared for achieving both rectifier and inverter operation. The switching signals, for power

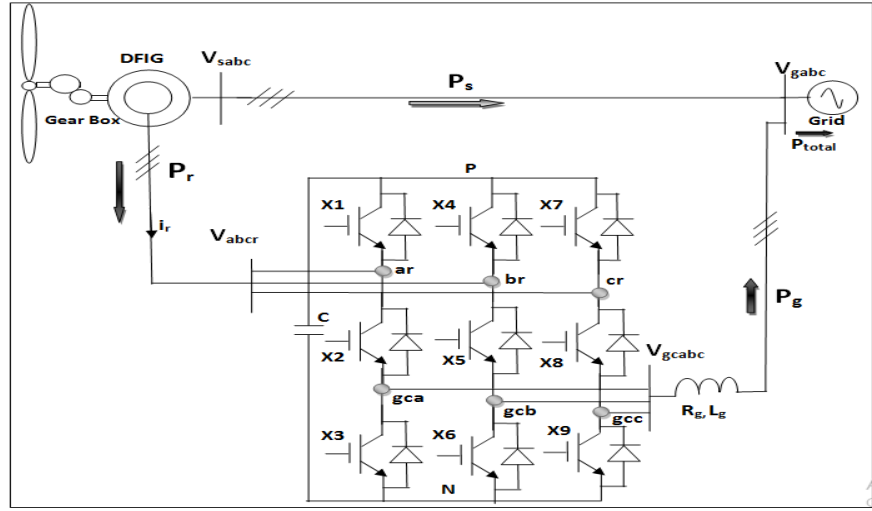


Fig.2: NSC based DFIG-WT System

Two modulating reference signals can be used for each phase, without intersecting each other, to overcome this limitation [IV]. In order to achieve this, the reference modulating signal for lower terminal of NSC should always be placed beneath that of the upper terminal of NSC with the inclusion of dc-offsets signals to both the modulating reference signals. The 120°-discontinuous modulation [I, XV] based modified reference modulating voltage signals for controller of NSC is given as follows:

$$\left. \begin{aligned} V_{abcr}^{*+} &= V_{abcr}^{*} + [1 - \max(V_{abcr}^{*})] \\ V_{gcabc}^{*+} &= V_{gcabc}^{*} - [1 + \min(V_{gcabc}^{*})] \end{aligned} \right\} \quad (1)$$

The three phase grid voltage reference, V_{gcabc}^{*} , is regulated by using grid-voltage-oriented vector control technique [XX] in order to control NSC to get decoupled control of: (i) active power flow between grid and dc-link capacitor using d-axis current component, to track the reference value of dc-link voltage (V_{dc}) and (ii) the reactive power flow, between GSC and grid, is controlled by regulating q-axis current component. The active component of grid power and hence the voltage across dc-link capacitor is directly proportional to d-axis current between GSC and Grid (i_{dg}), and is controlled by regulating V_{dgc}^{*} while the reactive grid power is directly proportional to q-axis current between GSC and Grid (i_{qg}) and is controlled by regulating V_{qgc}^{*} . In usual operating mode, the i_{dg}^{*} (reference d-axis current of GSC), is produced by means of dc-link voltage error (different between reference and actual voltages across DC-link capacitor) and DC-link voltage PI controller whereas the i_{qg}^{*} (q-axis reference current of GSC), is set to zero for achieving unity displacement factor (UDF) operation.

The three phase rotor voltage reference, V_{abcr}^{*} , is generated by using stator field oriented vector control approach to design upper part of the NSC control scheme for achieving variable speed operation under varying wind velocity. Stator field oriented vector control scheme is implemented in synchronously rotating dq-axis frame, with d-axis oriented along stator-flux vector position, for controlling the active power flow between the DFIG (stator and rotor) and the grid via NSC for tracking the MPP of the WT. The

detailed mathematical modelling of stator field oriented vector control approach is discussed in [XX]. The converter is current regulated with the qd-axis of rotor currents applied to control the stator active and reactive powers respectively. The stator active and reactive powers are proportional to i_{qr} and i_{dr} respectively and can be controlled by controlling V_{qr}^* and V_{dr}^* as shown in Fig.3. The qd-axis reference rotor current, i_{qr}^* and i_{dr}^* , are produced by means of stator active and reactive power based PI controllers respectively, as shown in Fig.3.

In B2B converter, the modified modulating reference signals (V_{gcabc}^{*st} & V_{abcr}^{*st}) are used to generate PWM based switching signals for the GSC and RSC converters. In case of NSC, the switching signals for middle three switches of NSC are produced by logical EX-OR process of the switching signals of upper and lower IGBT based power switches, by using the following relation: $X2=X1' \oplus X3'$ where $X1'$ and $X3'$ are the logical NOT operation of $X1$ and $X3$ and \oplus is the logical XOR operation.

IV. SIMULATION RESULT

To compare the effectiveness of the NSC in grid connected DFIG-WT system with that of B2BC for the same system under varying wind velocity; controllers have been designed and an extensive simulation study of the study system is carried out using MATLAB/Simulink software.

The time responses of essential state variables of DFIG-WT system have been obtained, first using B2BC and then using NSC-based system, to study the effectiveness of NSC for the system in comparison with B2BC. The performances have been presented: (1) in sub-section A for B2BC and (2) in sub-section B for NSC, for variation in wind velocity from rated to below rated and return back to rated (12 m/s is the rated wind speed). The system performances have been compared in section-VI.

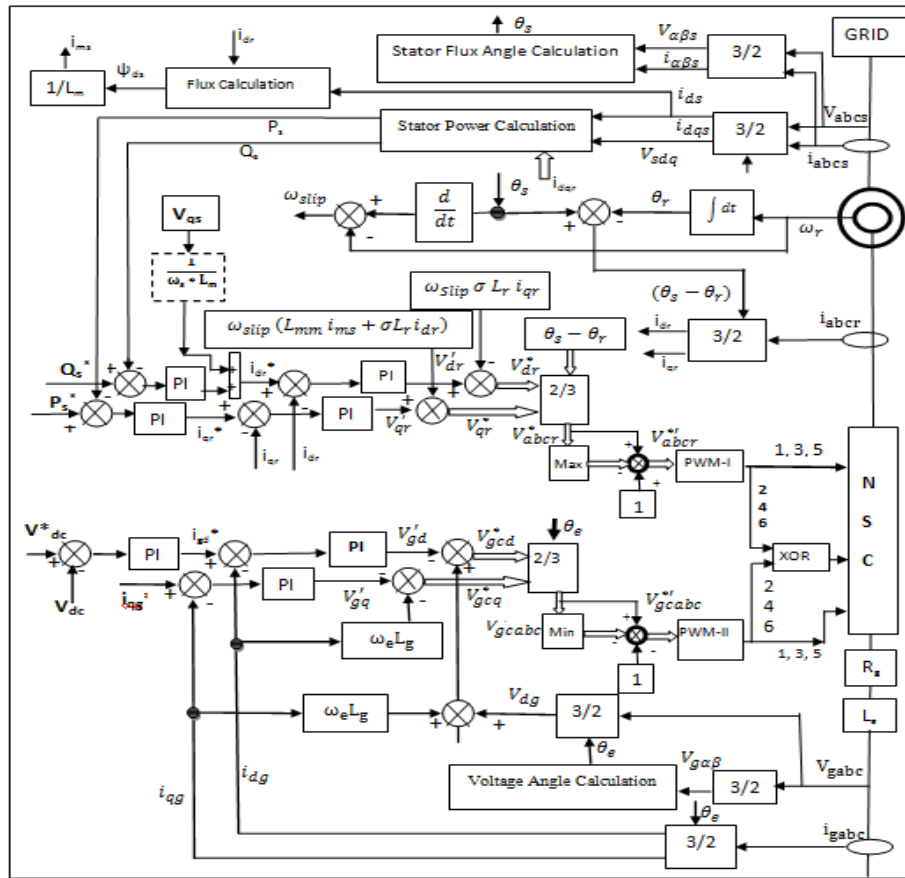


Fig.3 Control scheme for NSC

A. Simulation results of DFIG-WT system with B2BC

In this sub-section, steady state and transient responses of the system have been presented using B2BC when the system is subject to variation of wind velocity, as shown in Fig-4(a).

During 0 to 5 sec and 14 to 20 sec: wind velocity is 12m/s [Fig.4(a)]. Simulation result shows [Fig. 4(b-d)] that the active power based PI-controller adjusts the rotor speed of the generator to maintain rated power coefficient (C_p) to track the maximum rated power. In this interval, the DFIG operates at super-synchronous operation mode and hence, the rotor active power delivers to the grid from the rotor circuit (Fig-4(k) shows the direction of rotor active under super-synchronous mode of operation).

During 5 to 6 sec and 13 to 14 sec: wind velocity is considered to decrease from rated (12 m/s) to below rated (8 m/s) and increase from 8 m/s to 12 m/ in ramp. NSC controls the generator rotor speed to extract maximum of wind energy from the wind at that speed. Simulation results show that controller changes the generator operation from one operating mode to another operating mode i.e. from super to sub-synchronous mode of operation and vice versa. Hence, the active rotor power is fed to

the rotor windings from grid via NSC and to the grid from the rotor via NSC as shown in (Fig-4(k)).

During 6 to 13 sec: wind speed remains constant during time interval 6 to 13 sec i.e. 8m/s and the generator operates at sub-synchronous operation mode as illustrated in Fig.(K).

Also, the phase of rotor voltage is changed, as shown in Fig-4(m), while the rotor speed changes from super-synchronous to sub-synchronous and vice-versa. The unity power factor (UPF) operation is achieved by regulating zero reactive power exchange between grid and generator as shown in Fig.4.(f).

The MPPT controller forces the system to track the reference value, C_{p-max} corresponding to wind velocity of 12 m/s. However, a small deviation exists in C_p value during transient period.

The active power PI controller controls the rotor q-axis current for controlling the stator active power, electromagnetic torque and generator rotor speed corresponding to its desire values under the variation in wind velocity. To achieve UPF power generation, the rotor d-axis current is regulated by controlling the stator reactive power based PI controller at fixed value of stator /grid) voltage (V_{qs} =magnitude of grid/stator voltage with V_{ds} =zero) level.

The d-axis current of GSC is regulated by controlling dc-link based PI controller to maintain constant V_{dc} , shown in Fig. 4(m, n & p). The q-axis current of GSC is controlled to maintain injection of reactive power into grid is exactly equal to zero.

Although the steady state response of MPPT controller at any of the constant wind velocities ($V_w \leq V_{wrated}$) is found to be good, a deviation has been observed to exists in the value of C_p during transient interval. In true sense, the transient response of MPPT controller is found to be slightly sluggish. This resulted in the deviation in tracking the speed of rotation by rotor and active power by stator [Fig-4(b,d)]. A major reason for the sluggish transient response of MPPT controller may be due to the presence of high inertia of rotating mechanical components of the system.

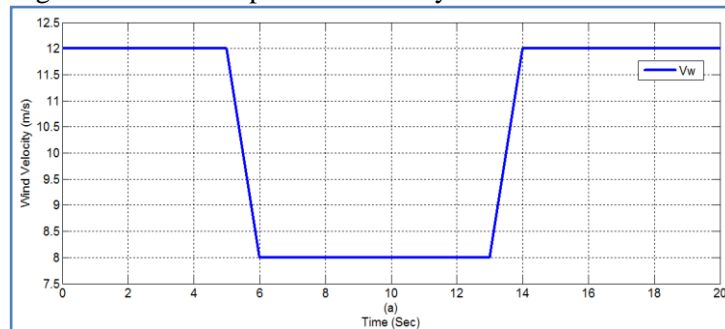


Fig-4(a) Wind Velocity (V_w)

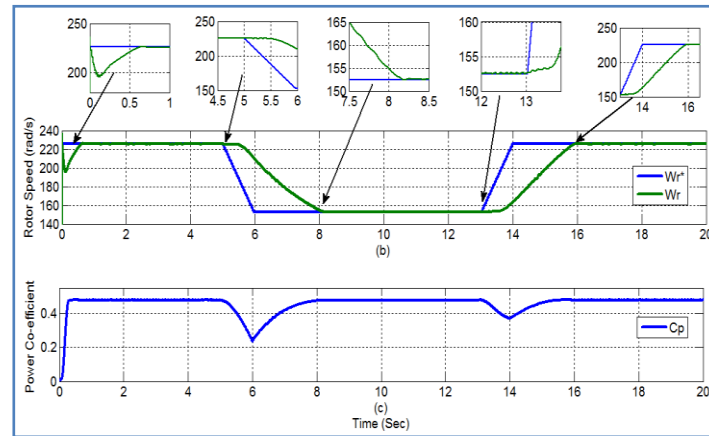


Fig.4 (b) Reference and actual generator speed (w_r^* & w_r) and (c) C_p

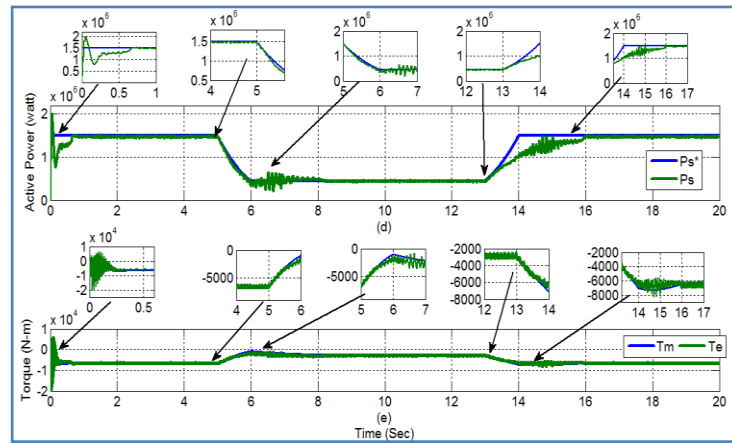


Fig.4(d) Reference & Active power from stator (P_s^* & P_s) and (e) Mechanical & Electrical Torque (T_m & T_e)

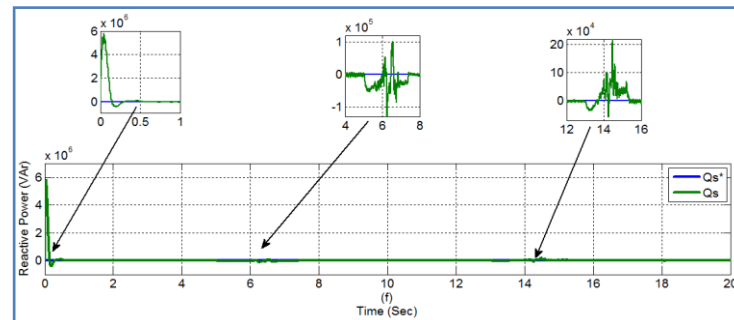


Fig.4 (f) Reference and Reactive power from stator (Q_s^* & Q_s)

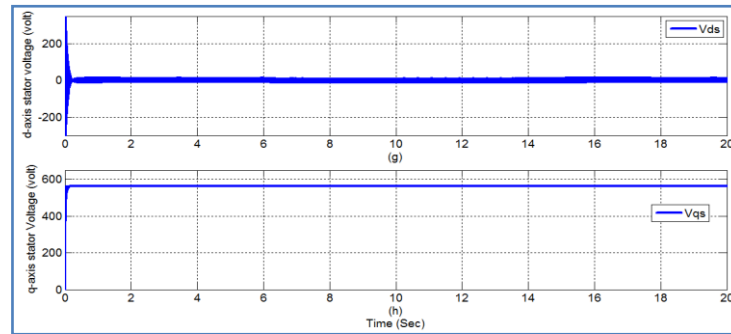


Fig.4 Stator voltage (g) d-axis component (V_{ds}) and (h) q-axis component (V_{qs})

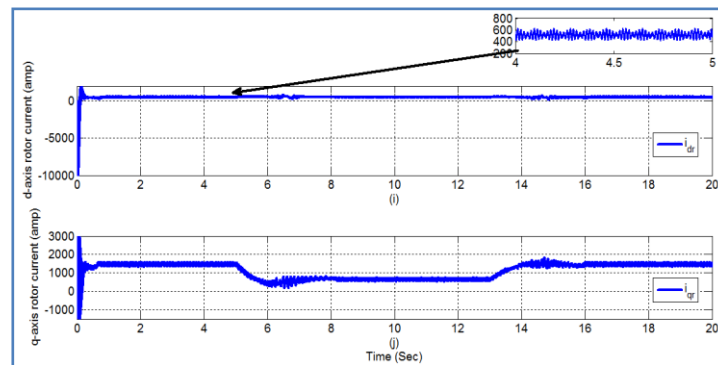


Fig.4 Rotor current (i) d-axis component (i_{dr}) and (j) q-axis component (i_{qr})

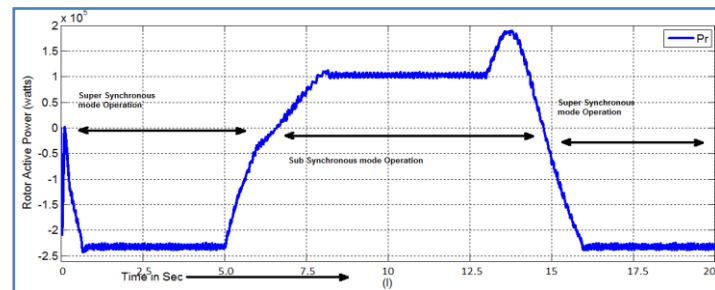


Fig.4(k) Active Power through Rotor (P_r)

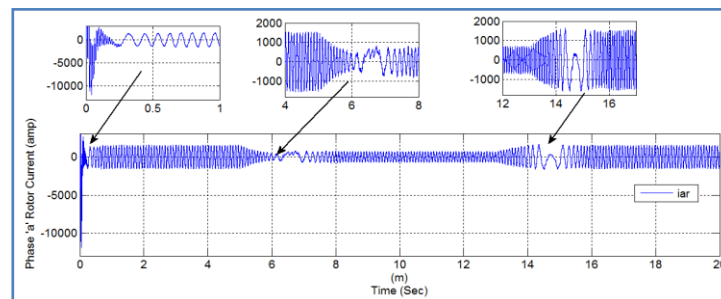


Fig.4(l) Waveform of one phase of Rotor current

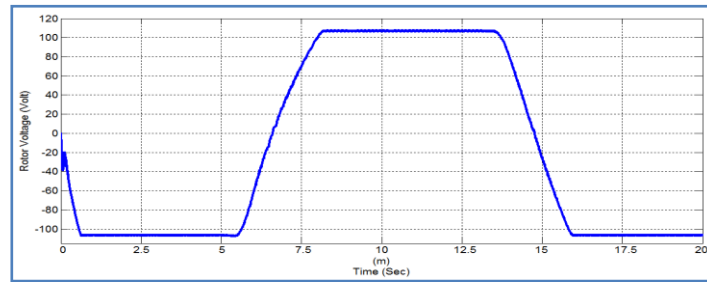


Fig.4 (m): Rotor Voltage (V_r)

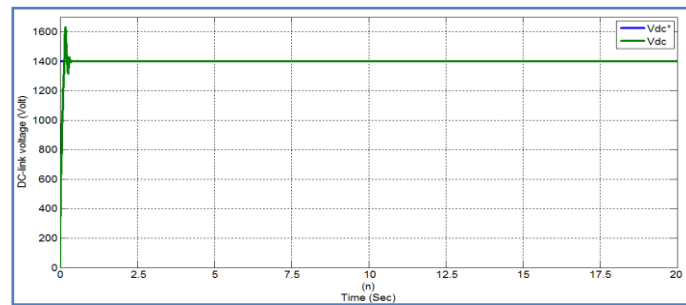


Fig.4(n) DC-link Voltage V_{dc}

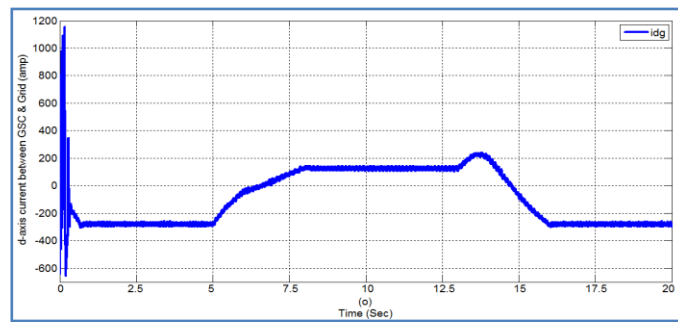


Fig.4(o) d-axis current between GSC and grid

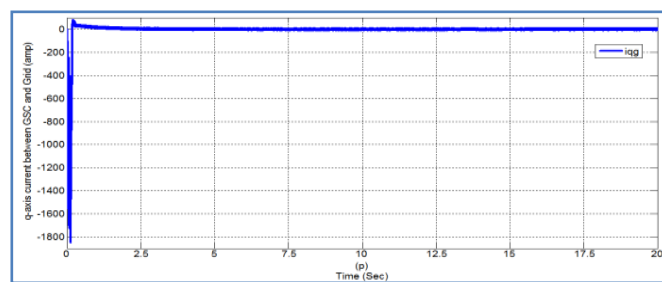


Fig.4(p) q-axis current between GSC and grid

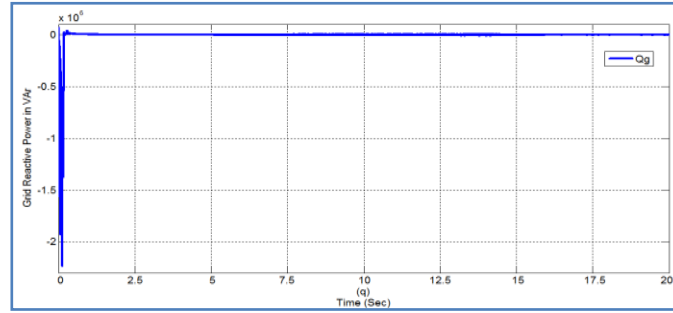


Fig.4(q) Grid Reactive Power (Q_g)

B. Simulation results and analysis of the NSC-based DFIG-WT system

In this sub-Section, steady state and transient responses of the system have been presented with NSC when the system is subjected to similar kind of wind velocity variation as considered for B2BC, i.e., first wind velocity varies from 12 m/s-to-8m/sec-to-12 m/s, as shown in Fig-5(a). From the simulation results, it may be noted that under steady state

- When wind velocity, $V_w = V_{w, \text{rated}}$:
 - Rotor of DFIG runs at super-synchronous speed, i.e., $\omega_r > \omega_s$, [Fig-5(b)].
 - C_p attains the desired level, $C_{p, \text{opt}} (= 0.48)$ [Fig-5(c)] and remains fixed at that level indicating the performance of MPPT controller.
 - Rated active power is delivered from stator to the grid ($P_s \approx P_{\text{rated}}$) [Fig-5(d)] at $Q_s = 0$ [Fig-5(f)],
 - P_r is +ve [Fig-5(k)], i.e., rotor absorbs active power from grid at $i_{dr} = \frac{V_s}{\omega_s L_m} = \frac{V_{qs}}{\omega_s L_m}$ [Fig. 5(i)], i.e., at $Q_s=0$.
- When wind velocity, $V_w < V_{w, \text{rated}}$:
 - Rotor of DFIG runs at sub-synchronous speed, i.e., $\omega_r < \omega_s$, [Fig-5(b)],
 - C_p attains the desired level, $C_{p, \text{opt}} (= 0.48)$ [Fig-5(c)] & remains fixed at that level,
 - Active power delivered from stator to the grid decreases below rated value, i.e., $P_s < P_{\text{rated}}$ [Fig-5(d)] at $Q_s = 0$ [Fig-5(f)].
 - P_r is +ve [Fig-5(k)], i.e., rotor absorbs active power from grid at $i_{dr} = \frac{V_s}{\omega_s L_m} = \frac{V_{qs}}{\omega_s L_m}$ [Fig. 5(i)], i.e., at $Q_s=0$.
- The voltage across DC-link capacitor [Fig-5(m)] is found to remain fixed to its rated value irrespective to the change in wind speed. This indicates the quality of performance of the controller for GSC.
- The change in the direction of rotor power can be visualised from the waveform of rotor voltage also, as shown in Fig-5(k). It may be noted that the rotor current changes phase at two instants (at around 6.5 sec & 14.6 sec) of time. The phase change occurs due to the change of rotor speed from super-synchronous to sub-synchronous and vice-versa [shown in Fig-5(b)] causing corresponding changes in the direction of flow of rotor power, P_r as shown in Fig-5(k). This is also observed with the change of sign of the rotor voltage as shown in Fig-5(m).

- In this case, like earlier case, a deviation is also observed in the value of C_p , speed of rotation by rotor and active power by stator while tracking their reference values during transient intervals (especially when subjected to ramp increase/decrease) [Fig-5(b)-(d)]. Transient responses of C_p , ω_r & P_s during changes in wind velocity are found to be sluggish. However, transient responses of all other variables are good.

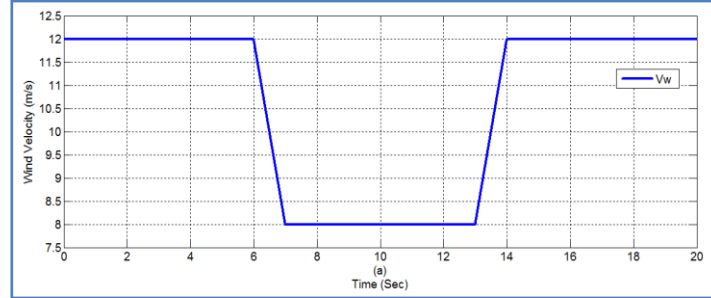


Fig.5: (a) Wind Velocity

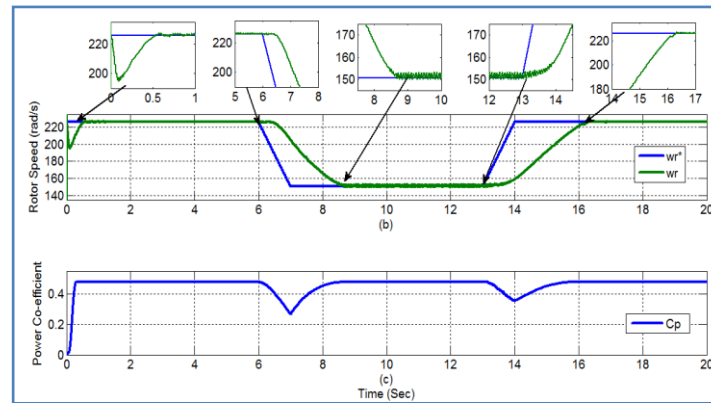


Fig-5: (b) Reference & actual generator speed (w_r^* & w_r) and (c) C_p

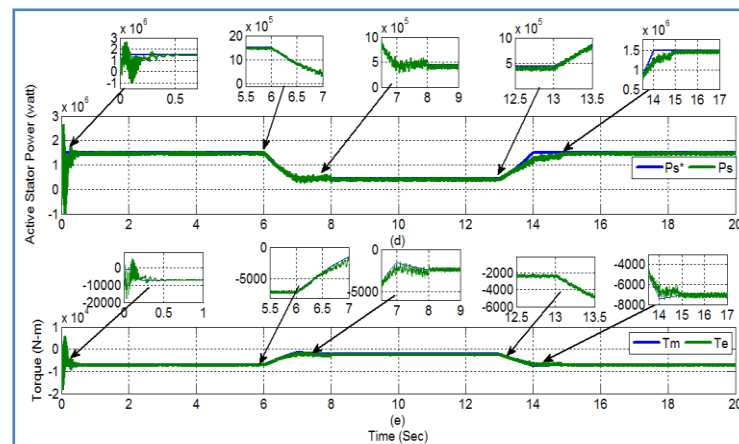


Fig.5: (d) Reference & Actual active power (P_s^* , P_s) and (e) Mechanical & Electrical Torque (T_m & T_e)

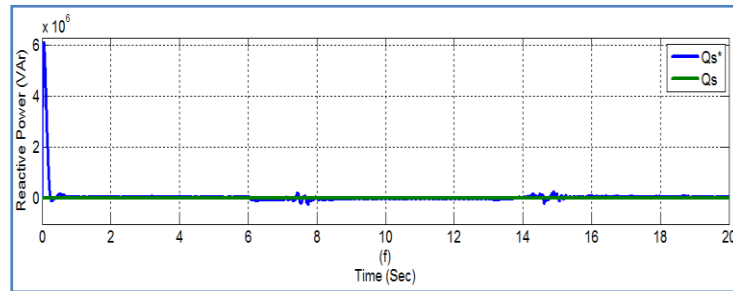


Fig.5: (f) Reference & Actual reactive power (Q_s^* , Q_s)

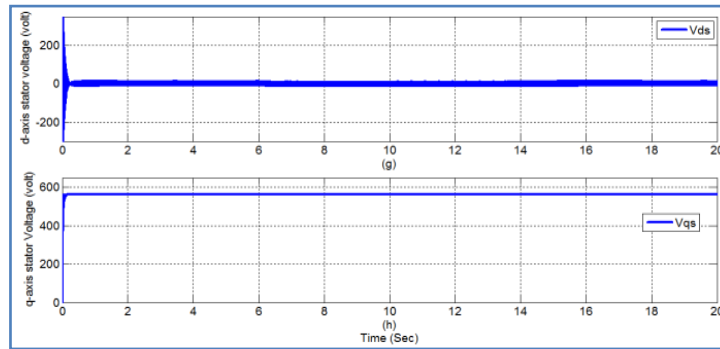


Fig.5: Stator voltage (g) d-axis component (V_{ds}) and (h) q-axis component (V_{qs})

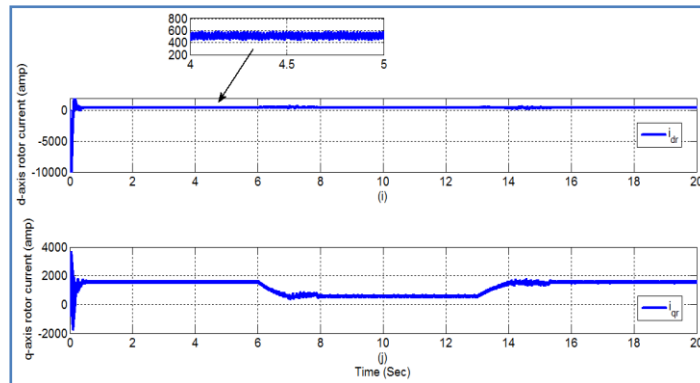


Fig. 5: (i) d-axis rotor current (i_{dr}) and (j) q-axis rotor current (i_{qr})

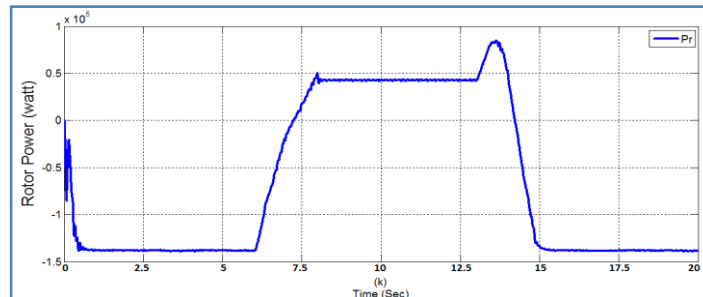


Fig.5: (k) Rotor Power (P_r)

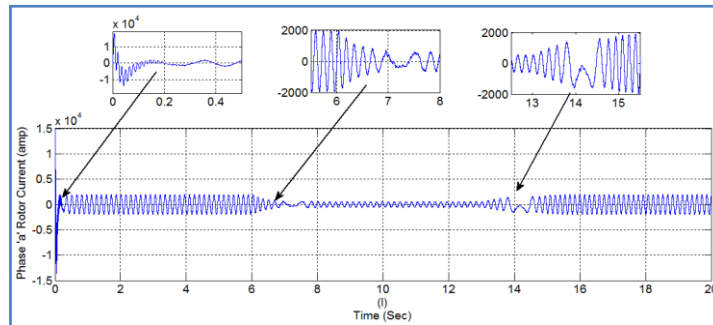


Fig.5: (l) Current waveform of one of the phases of rotor

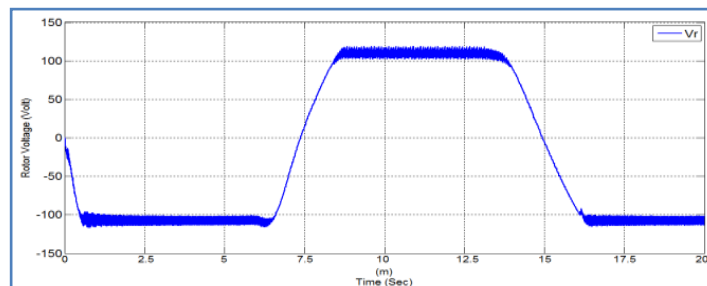


Fig. 5: (m) Rotor Voltage (V_r)

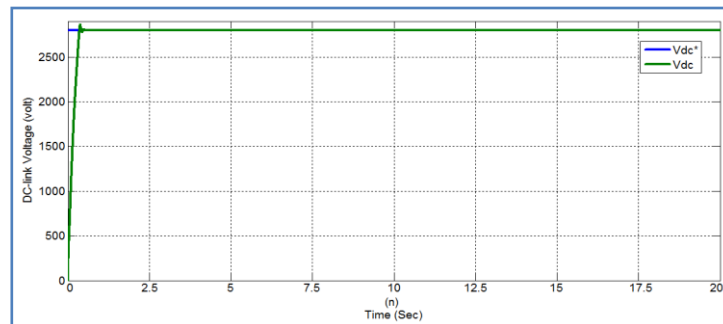


Fig. 5: (n) DC-link Voltage

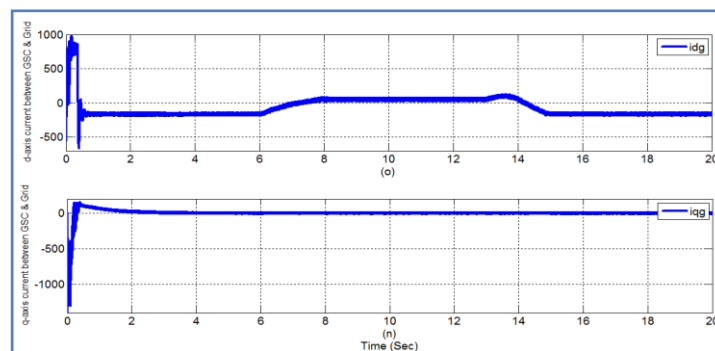
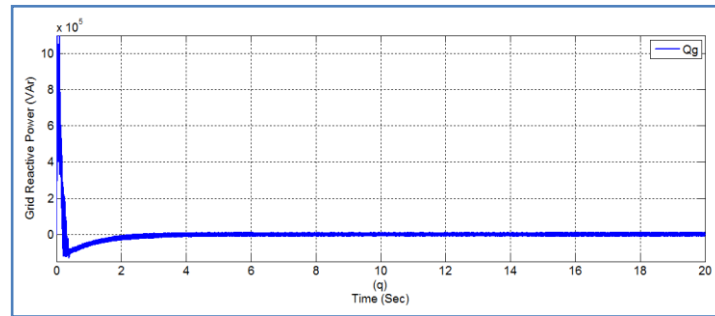


Fig.5: (n) d-axis and (o) q-axis currents of GSC & Grid

Fig.5: (p) Reactive power (Q_g) between GSC & Grid

V. COMPARISON OF THE SYSTEM PERFORMANCE

Converter performance is decided by the time-response of the system in which it is used. Time responses of the system with B2BC as well as those with NSC have been presented in section-V.

The results obtained in section-V, using the two types of converters, are listed in Table-II along with comments on the responses obtained with the two types of converters.

Table-II: Comparison of system responses with B2BC & NSC controllers

Variables	Fig No		Comments on system response with two controllers when speed of wind varies from 12m/s to 8m/s and return back 12m/s
	With B2BC	With NSC	
V_w	4(a)	5(a)	Same type of wind velocity has been applied in both the cases.
ω_r	4(b)	5(b)	Steady state responses obtained with both types of converters & controllers are equally good. Transient responses w.r.t. rise time, settling time etc. are almost same.
C_p	4(c)	5(c)	The time responses of power co-efficient are almost same for both converters.
P_s	4(d)	5(d)	The time responses of active power are same in both the cases, but few oscillations were observed to occur in the transient responses with B2BC before steady state is reached.
T_e	4(e)	5(e)	The time responses of torque are almost same.
Q_s	4(f)	5(f)	The time responses of reactive power with both converters are almost same.
i_{dr}	4(i)	5(i)	Both the control schemes of NSC have tracked the value of $i_{dr} = \frac{V_s}{\omega_s L_m} = \frac{V_{qs}}{\omega_s L_m}$ under steady as well as transient states, to generate active power at UPF by compensating on load magnetizing reactive power drawn from the grid.
i_{qr}	4(j)	5(j)	Both the converters and controllers have perfectly tracked the reference values of i_{qr} as required.

P_r	4(k)	5(k)	The time responses of rotor active power with and without speed sensor are almost same.
V_{dc}	4(m)	5(m)	Both the converters have perfectly tracked the reference values of V_{dc} and kept it fixed to that level.
Q_g	4(p)	5(p)	Both the converters and controllers have perfectly tracked the reference values of $Q_g=0$ for unity power factor operation.

VI. CONCLUSIONS

Performance of a 1.5MW grid connected DFIG-WT system has been obtained by replacing B2BC with NSC. The system performance with NSC has been compared with that obtained using B2BC. The time domain responses illustrate that DFIG-WT system with NSC can work according to control scheme aimed at and can offer good dynamic response under any wind velocity. It has also been observed that, like B2BC, the NSC is sufficiently capable to achieve decoupled control of active and reactive power for ensuring capture of maximum wind power and transmit the same at UPF under varying wind speeds. So, it can be concluded that the NSC can successfully replace B2BC and reduce the switching losses and cost of the system.

References

- I. A. M. Hava, R. Kerkman, and T. A. Lipo, "Carrier-based PWM-VSI over modulation strategies: analysis, comparison, design," IEEE Transactions on Power Electronics, Vol. 13, no.4, July 1998, pp. 674–689.
- II. B. H. Chowdhury, S. Chellapilla, "Double Fed Induction Generator Control for Variable Speed Wind Power Generation," Elsevier Power System Research, Vol.76, pp: 786-800, 2006.
- III. C. Liu, B. Wu, N. R. Zargari, D. Xu, and J. Wang, "A novel three phase three-leg ac/ac converter using nine IGBTs," IEEE Trans. Power Electron., vol. 24, pp. 1151–1160, 2009.
- IV. C. Liu, B. Wu, N. Zargari and D. Xu, "A novel nine-switch PWM rectifier-inverter topology for three-phase UPS applications," Journal of European Power Electronics (EPE), vol. 19, pp. 1 -10, 2009.
- V. C. Klumpner and F. Blaabjerg, "Experimental evaluation of ride-through capabilities for a matrix converter under short power interruptions," IEEE Trans. Industrial Electronics, Vol. 49, pp. 315-324, 2002.
- VI. F. Blaabjerg, S. Freysson, H. H. Hansen, and S. Hansen, "A new optimized space-vector modulation strategy for a component-minimized voltage source inverter," IEEE Trans. Power Electron., vol. 12, pp. 704–714, 1997.
- VII. F. Gao, L. Zhang, D. Li, P.C. Loh, Yi Tang and H. Gao, "Optimal pulse-width modulation of nine-switch converter," IEEE Transaction on Power Electronics, vol. 25, pp. 2331-2343, 2010.

- VIII. G. Li, M. Yin, M. Zhou and C. Zhao, "Decoupling control for multi terminal VSC HVDC based wind farm interconnection," IEEE Power Engineering Society General Meeting, pp.1-6, 2007.
- IX. Gui-Jia Su Hsu, J.S., "A five-leg inverter for driving a traction motor and a compressor motor," IEEE Transactions on Power Electronics, vol. 21, pp. 687 - 692, 2006.
- X. H. Nikkhajoei, R. H. Lasseter, "Power quality enhancement of a wind-turbine generator under variable wind speeds using matrix converter," Power Electronic Specialists Conference, pp. 1755-1761, 2008.
- XI. Lie Xu, "Coordinated Control of DFIG's Rotor and Grid Side Converters during Network Unbalance," IEEE Trans. on Power Electronics, Vol. 23, pp.1041-1049, 2008.
- XII. L. Holdsworth, X. G. Wu, J. B. Ekanayake and N. Jenkins, "Comparison of fixed speed and doubly-fed induction wind turbines during power system disturbances," IEE Proc. Gener. Transm. Distrib., Vol. 150, pp. 343-352, 2003.
- XIII. M.V.A. Nunes, H.H. Zurn, U.H. Bezerra, J.A. Pecas Lopes, R.G. Almeida, "Influence of the variable Speed wind Generators in Transient Stability Margin of the Conventional Generators Integrated in Electrical Grids," IEEE Transactions on Energy Conversion, Vol. 21, pp.257-264, 2006.
- XIV. M. Jones, S. N. Vukosavic, D. Dujic, E. Levi, and P. Wright, "Five-leg inverter PWM technique for reduced switch count two-motor constant power applications," IET Proc. Electric Power Application, vol. 2, pp. 275–287, 2008.
- XV. O. Ojo, "The generalized discontinuous PWM scheme for three phase voltage source inverters," IEEE Trans. Ind. Electron., vol.51, pp.1280-1289, 2004.
- XVI. P. C. Loh, F. Blaabjerg, F. Gao, A. Baby, and D. A. C. Tan, "Pulse width modulation of neutral-point-clamped indirect matrix converter," IEEE Trans. Ind. Application, vol. 44, pp. 1805–1814, 2008.
- XVII. R.G. Almeida, E.D. Castronuovo, J.A. Pacas Lopes, "Optimum Control in Wind Parks when Carrying out system Operator Requests," IEEE Transactions Power System. Vol.19, pp 1942-1950, 2006.
- XVIII. R. Cardenas, R. Pena, G. Tobar, J. Clare, P. Wheeler, G. Asher, "Stability Analysis of a Wind Energy Conversion System Based Doubly Fed Induction Generator Fed By a Matrix Converter," IEEE Trans. on Industrial Electronics, Vol. 56, pp.4194-4206, 2009.
- XIX. S. Datta, J. P. Mishra and A. K. Roy, "Modified Speed Sensor-less Grid Connected DFIG based WECS", Indian Journal of Science of Technology, Vol. 8, Issue No. 16, pp.1-12, 2015.
- XX. S. Datta, J. P. Mishra and A. K. Roy, "Operation and control of a DFIG-based grid-connected WECS using NSC during grid fault and with unbalanced non-linear load", International Journal of Ambient Energy, Vol.39, No.7, pp.732-742, 2018.
- XXI. T. Kominami and Y. Fujimoto, "A novel nine-switch inverter for independent control of two three-phase loads," IEEE Industry Applications Society Annual Conference (IAS), pp. 2346-2350, 2007.
- XXII. Y. Lei, A. Mullane, G. Lightbody, R. Yacamini, " Modeling of the wind turbine with a Doubly fed Induction Generator for Grid Integration Studies," IEEE Transactions on Energy Conversion, Vol. 21, pp.257-264, 2006.
- XXIII. Z. Lei, P. C. Loh and F. Gao, "An integrated nine-switch power conditioner for power quality enhancement and voltage sag mitigation," IEEE Transaction on Power Electronics, vol. 27, pp. 1177-1190, 2012.